Expression, purification and crystallization of the (3R)-hydroxyacyl-ACP dehydratase HadAB complex from *Mycobacterium tuberculosis*

CrossMark

Yu Dong [a,b,1], Jun Li [a,1], Xiaodi Qiu [a,b], Chuanqiang Yan [a,b], Xuemei Li [a,*]

[a] National Laboratory of Biomacromolecules, Institute of Biophysics, Chinese Academy of Sciences, 15 Datun Road, Beijing 100101, People's Republic of China
[b] University of Chinese Academy of Sciences, Beijing 100049, People's Republic of China

ABSTRACT

The (3R)-hydroxyacyl-ACP dehydratase HadAB, involved in the biosynthetic pathway for mycolic acid (MA) of *Mycobacterium tuberculosis*, catalyzes the third step in the fatty acid (FA) elongation cycle, which is an ideal and actual target for anti-tubercular agent. Though HadAB is predicted to be a member of the hotdog superfamily, it shares no sequence identity with typical hotdog fold isoenzyme FabZ. To characterize the significance of HadAB from the perspective of structural biology, large amount of pure HadAB complex is required for biochemical characterization and crystallization. Here, we used a unique expression and purification method. HadA and HadB were cloned separately and co-expressed in *Escherichia coli*. After GST affinity chromatography, two steps of anion exchange chromatography and gel filtration, the purity of the protein as estimated by SDS–PAGE was >95%. Using hanging-drop vapor-diffusion method, crystals were obtained and diffracted X-rays to 1.75 Å resolution. The crystal belongs to space group $P4_12_12$, with unit-cell parameters $a = b = 82.0$ Å, $c = 139.8$ Å, $\alpha = \beta = \gamma = 90.0°$.
© 2015 The Authors. Published by Elsevier Inc. This is an open access article under the CC BY-NC-ND license (http://creativecommons.org/licenses/by-nc-nd/4.0/).

1. Introduction

Tuberculosis (TB), caused by *Mycobacterium tuberculosis* (*Mtb*), is the second most common cause of death due to a single infectious pathogen with an enormous global medical burden [1,2]. The complicated cell envelope of *Mtb* contains many kinds of lipids which play vital roles in the physiology and pathogenicity of this bacterium [3,4]. Mycolic acids (MAs), 2-alkyl, 3-hydroxy long-chain (C_{60}–C_{90}) fatty acids, constitute the major and specific lipid component of the envelope. They either link covalently to the cell wall peptidoglycan via the underlying arabinogalactan to form Mycolic acid–Arabinogalactan-Peptidoglycan complex (MAPc) or exist in the mycomembrane as trehalose mono- and dimycolates [5]. This provides a thick layer of lipid in the cell wall and protects the Mtb from dry environment, poisonous chemicals and host's immune system [6,7].

The biosynthetic pathway of this MAs involves two types of fatty acid-synthesizing systems (FASs): the multifunctional FAS-I and the dissociated FAS-II [8] (Fig. 1). The latter is composed of a series of discrete soluble enzymes which act successively and repetitively to elongate the FA chains produced by FAS-I [7]. There are four kinds of enzymes catalyze each cycle of elongation in *Mtb*: the β-ketoacyl-ACP synthetases (KasA and KasB, Rv2245 and Rv2246, respectively. Enzyme Classification No.: 2.3.1.41), the β-ketoacyl-ACP reductase (MabA, Rv1483. EC: 1.1.1.100), the β-hydroxyacyl-ACP dehydratases (HadAB and HadBC, Rv0635-Rv0636 and Rv0636-Rv0637. EC Number is not registered), and the trans-2-enoyl-ACP reductase (InhA, Rv1484. EC: 1.3.1.9). Deficiency or inactivation of anyone above will cease the biosynthesis of MA and absence of these enzymes in human make them very ideal and actual targets for drug discovery [9,10].

The (3R)-hydroxyacyl-ACP dehydratase HadAB, composed of two subunits HadA (Rv0635) and HadB (Rv0636), catalyzes the third step in the FA elongation cycle by dehydrating β-hydroxyacyl-ACP to trans-2-enoyl-ACP, which is the last piece to be identified in the mycobacterial FAS-II [11]. HadAB would take part, like KasA, in the early FA elongation cycles, leading to the formation of the intermediate-size (C_{32}–C_{42}) meromycolic chains, while HadBC, like KasB, would elongate further the intermediate-size meromycolic chains to full-size molecules (C_{52}–C_{64}) during the late elongation cycles [11,12]. It has been verified that NAS-21, NAS-91, some kinds of flavonoids and an anti-TB prodrug Thiacetazone (TAC) can inhibit the activity of HadB (Rv0636) as well as the growth of bacteria at different levels by mutation and overexpression methods [13–16]. Therefore HadAB complex is a significant drug target.

Though HadAB is predicted to be a member of hotdog superfamily, it resides only in *Corynebacterineae* and presents a different

---

* Corresponding author.
  E-mail address: lixm@sun5.ibp.ac.cn (X. Li).
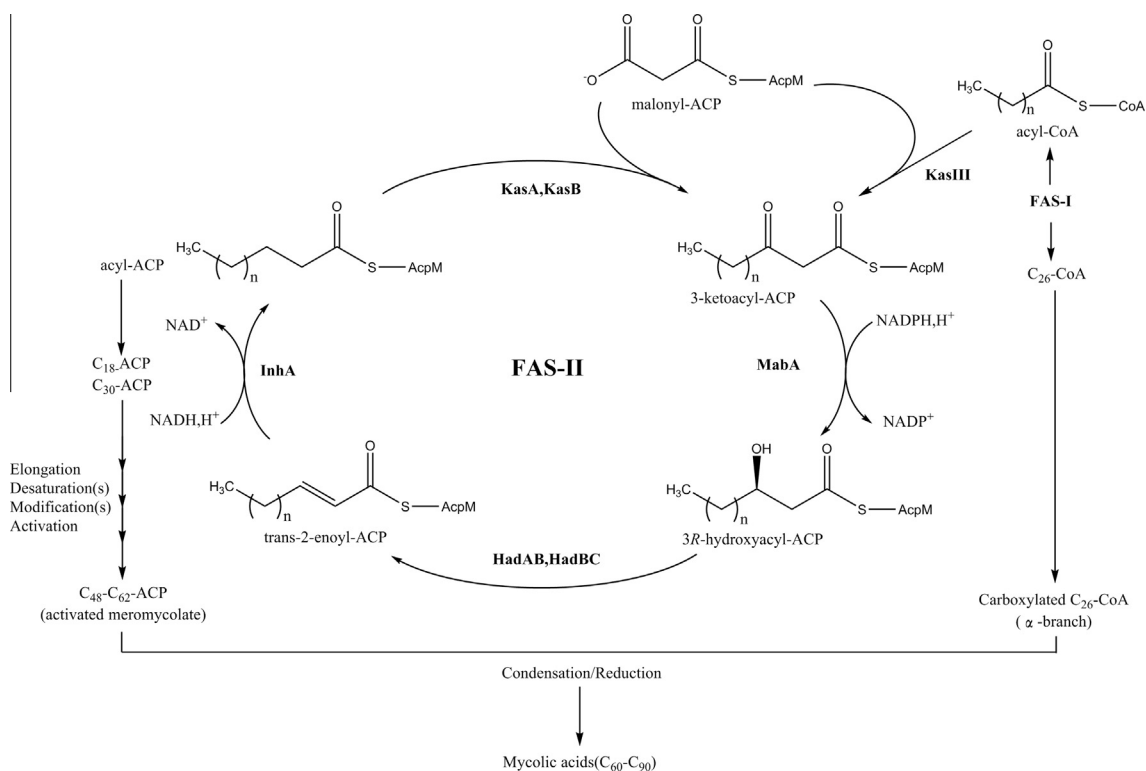[1] These authors contributed equally to this work.

Fig. 1. Biosynthetic pathway of mycolic acids in *M. tuberculosis*. AcpM: mycobacterial acyl-carrier-protein involved in FAS-II system.

Table 1
Summary of purification conditions of HadAB.

Parameters	GST affinity	HiTrap™ Q HP	RESOURCE™ Q	Superdex 75
Column volume	2 mL	5 mL	1 mL	24 mL
Buffer	Buffer A (50 mM Tris–HCl, pH 8.0, 300 mM NaCl and 10% (v/v) glycerol)	Buffer B (50 mM Tris–HCl, pH 8.0, 50 mM NaCl and 10% (v/v) glycerol) Buffer C (50 mM Tris–HCl, pH 8.0, 1 M NaCl and 10% (v/v) glycerol)		Buffer D (50 mM Tris–HCl, pH 8.0, 150 mM NaCl, and 10% (v/v) glycerol)
Sample volume	About 150 mL	50 mL	50 mL	Less than 500 μL
Flow rate	2 mL min^{-1}	1.5 mL min^{-1}	1.5 mL min^{-1}	0.5 mL min^{-1}
Washing volume	60–100 mL	10–15 mL	2–3 mL	–
Elution mode	After 30 μg mL^{-1} Prescission Protease treatment in 10 mL Buffer A overnight, directly collect the flow through	Elute with a linear gradient (0.05–0.5 M) of NaCl concentration in 40 mL	Elute with a linear gradient (0.05–0.45 M) of NaCl concentration in 8 mL	Elute with Buffer D

or distantly related catalytic sequence motif compared to the typical isoenzyme FabZ (EC: 4.2.1.59) which widely represented in other bacteria [11,17,18]. Currently, all of the resolved FabZ structures have similar hexametric hotdog fold structures, displaying a classic "trimer of homodimer" organization [19–22]. Because of the particular long substrate and failing to identify a specific mycobacterial homologue by BLAST searches of *E. coli* FabA (EC: 4.2.1.59 and 5.3.3.14) [17], another typical member of hotdog family [23], it seems possible that HadAB possesses new structural features to execute dehydration process. Determination of the crystal structure of HadAB would allow thorough understanding of the differences and similarities between HadAB and FabZ and lay the foundation for new anti-TB drug development.

In this work, because common or tandem expression could not get enough protein with high purity and stability for crystallization, a method for co-expression of the recombinant HadAB was developed. The gene of HadA and HadB was cloned respectively into different vectors, co-transformed into *E. coli* cells and the enzyme HadAB complex was expressed. Then we described the

purification, crystallization and preliminary X-ray diffraction analysis of HadAB from *Mycobacterium tuberculosis*. Our work provided a particular method of protein complex expression and purification and laid the foundation for structure determination of HadAB and more similar enzymic complexes.

2. Materials and methods

In this work, we used pGEX-6p-1, Glutathione Sepharose resin, HiTrap™ Q HP anion exchange column, RESOURCE™ Q anion exchange column and Superdex 75 10/300 GL gel-filtration column from GE Healthcare (USA); pRSFDuet-1 from Novagen (USA); SDS and isopropyl-β-d-thiogalactoside (IPTG) from Sigma (USA); tryptone, yeast extract and protein standards for electrophoresis from Thermo Fisher Scientific (USA); tris, glycine, DTT and Coomassie G-250 and R-250 from Amresco (USA); ultrafiltration equipment from Millipore (USA); crystallization screening kits from Hampton Research (USA); DNA extraction kit from QIAGEN
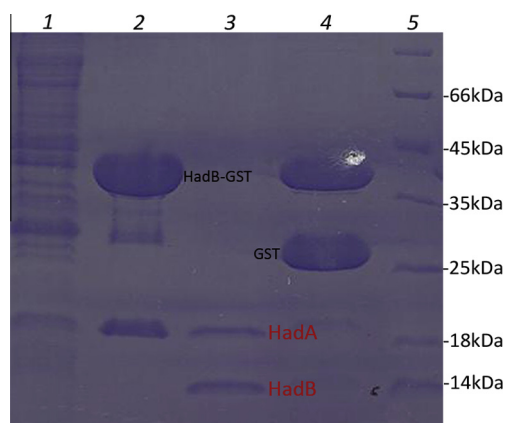
Fig. 2. SDS–PAGE analysis of HadAB during GST affinity purification. Lane 1, total proteins after flowing through from Glutathione Sepharose column; lane 2, the bound proteins enriched on the column, the GST tagged HadAB complex was the most; lane 3, the elution after Prescission Protease digestion overnight, the free untagged HadAB complex was eluted; lane 4, the resin after elution showed that the GST tag and the uncut GST-HadB were left on the column. This means the digestion was uncompleted; lane 5, molecular weight standard markers. HadAB was run on 16% SDS–PAGE and stained with Coomassie R-250 to estimate its purity (similarly hereinafter).
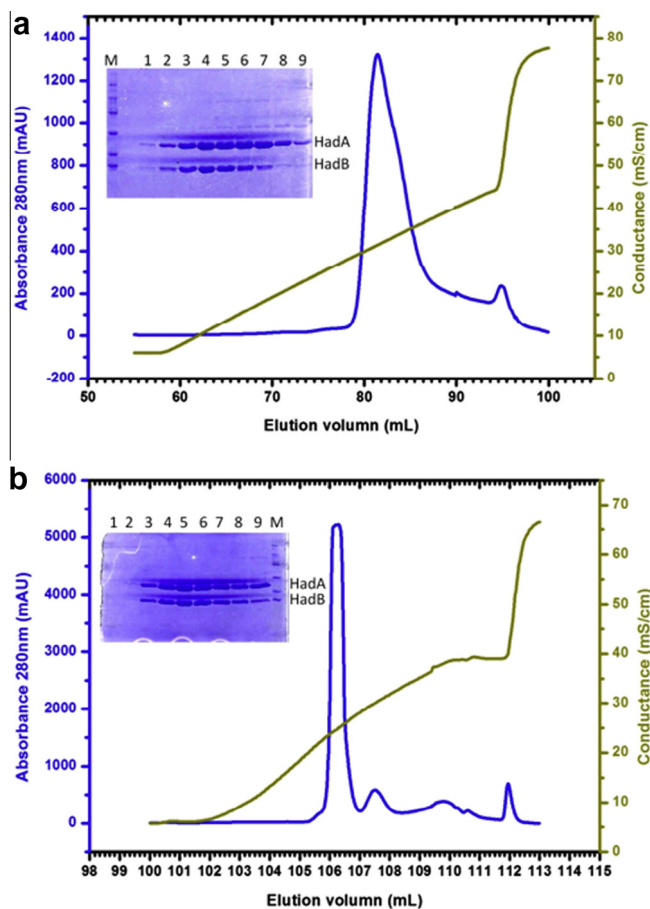

Fig. 3. SDS–PAGE analysis (inset) and elution profile of HadAB during ion exchange chromatography using a HiTrap™ Q HP anion exchange column (a) and a RESOURCE™ Q anion exchange column (b). In (a), lane 1–7 depict samples from elution volume 78.50–84.10 mL, 0.8 mL each; lane 8, sample between 84.9 and 85.7 mL; lane 9, sample between 86.5 and 87.3 mL. There are small amount of impure proteins in the elution samples under the peak. Thus, HadAB is not very pure. In (b), lane 1–9 depict samples from elution volume 105.4–107.2 mL, 0.2 mL each. The purity of HadAB under the peak is improved by the second ion exchange chromatography.
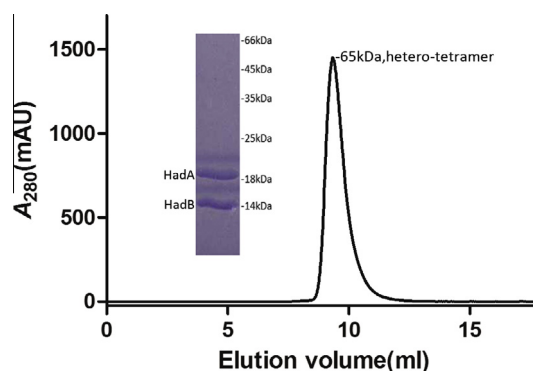

Fig. 4. SDS–PAGE analysis (inset) and elution profile of HadAB during gel filtration chromatography using a Superdex 75 column. The well-shaped single peak means the sample is homogenous. The final purity of sample after gel filtration as estimated by SDS–PAGE was >95%.

Table 2
Data collection statistics for HadAB.

Data collection	
Space group	$P4_12_12$
Unit-cell parameters	
a, b, c (Å)	$a = b = 82.0$, $c = 139.8$
α, β, γ (°)	$\alpha = \beta = \gamma = 90.0$
Wavelength (Å)	1.00000
Resolution (Å)	50.00–1.75 (1.81–1.75)[a]
Total observation	462,997
Unique reflections	48,837
Data completeness (%)	99.9 (100.0)
R_{merge}[b]	0.058 (0.424)
$I/\delta(I)$	35.8 (5.8)
Redundancy	9.5 (9.6)

[a] Values in parentheses are for the highest resolution shell.
[b] $R_{merge} = \Sigma_h\Sigma_i|I_{ih} - \langle I_h\rangle|/\Sigma_h\Sigma_i\langle I_h\rangle$, where $\langle I_h\rangle$ is the mean intensity of the observations of I_{ih} of reflection h.

(Germany); restrictase BamHI, NdeI, XhoI, T4 DNA ligase and corresponding buffer solution from TaKaRa(China).

All other reagents were of high purity or reagent grade (China).

2.1. Molecular cloning

The *Rv0635* gene encoding HadA was amplified from *M. tuberculosis H37Rv* genomic DNA by using ExTaq polymerase (TaKaRa) as well as the forward primer 5′- TTCCATATGGTGGCGTTGA GCGCAGACAT-3′ and the reverse primer 5′-CCGCTCGAGTCA CGCAGCGCCATCAGAAA-3′. NdeI and XhoI restriction sites are underlined. Amplification were carried out by a thermal cycler (Bio-Rad) according to the following protocol: step 1, 95 °C for 300 s; step 2, 94 °C for 40 s; step 3, 60 °C for 40 s; step 4, 72 °C for 32 s; repeat from step 2 for 30 cycles. The PCR products were subjected to a final amplification step of 5 min at 72 °C. They were separated by horizontal electrophoresis in 1% agarose gel. The product corresponding to HadA (about 500 bp) was extracted from the gel using the DNA extraction kit (QIAGEN). Then the purified PCR product was hydrolyzed with endonucleases NdeI and XhoI and ligated according to the manufacturer's protocol with expression vector pRSFDuet-1 (Novagen), which was preliminarily treated with the same endonucleases. The *Rv0636* gene from the same source which encodes HadB was PCR-amplified using primers pBm_F (5′-CGCGGATCCATGGCGCTGCGTGAGTTCAG-3′) and pXh_R (5′-CCGCTCGAGCTACGCTAACTTCGCCGAGG-3′). BamHI and XhoI restriction sites are underlined. Amplification protocol is the same as HadA. After restriction digestion, the gene was ligated into the
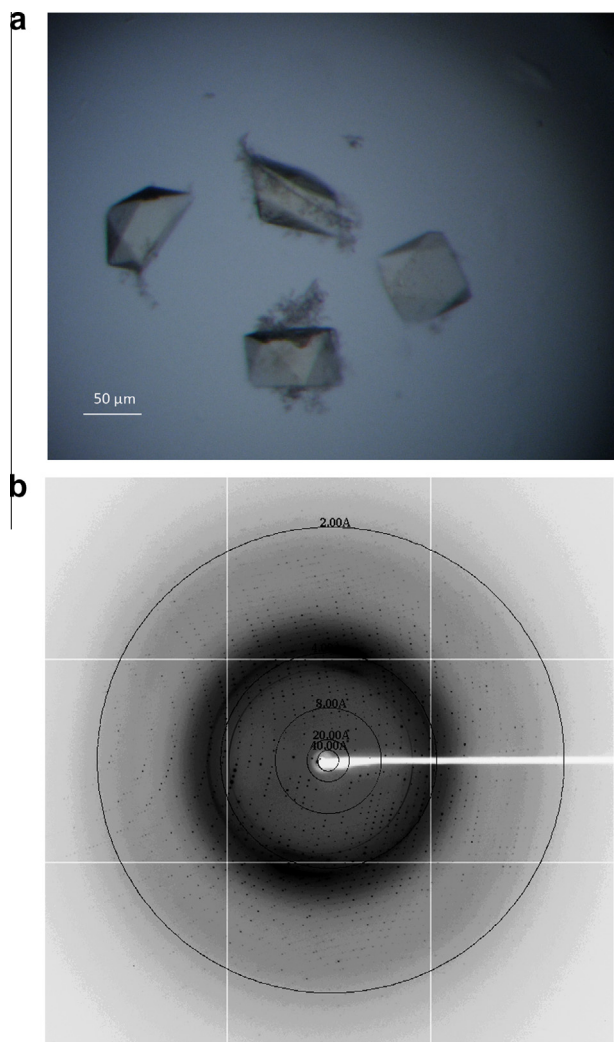
Fig. 5. (a) Typical crystals of HadAB suitable for collecting diffraction images under X-ray. (b) A typical X-ray diffraction image obtained from a crystal of HadAB complex. Resolution rings were marked.

pGEX-6p-1 vector (GE Healthcare). The recombinant plasmids pRSFDuet-1-HadA and pGEX-6p-1-HadB were co-transformed into *E. coli.* BL21(DE3) for expression. Correct clone was screened by bi-anti agar plate and PCR and confirmed by DNA sequencing.

2.2. Expression and purification of HadAB

For expression of GST-HadAB recombinant protein, the cells were grown aerobically at 37 °C in 2 L Terrific Broth medium with 100 $\mu g\,mL^{-1}$ ampicillin and 50 $\mu g\,mL^{-1}$ kanamycin. When the OD_{600} reached ~1.0, the culture was induced with 0.3 mM isopropyl-β-D-thiogalactopyranoside (IPTG, Sigma) and incubated at 16 °C for 18 h. Cells were harvested by centrifugation at 4200g for 30 min at 4 °C and resuspended in 160 mL Buffer A (50 mM Tris–HCl, pH 8.0, 300 mM NaCl, and 10% (v/v) glycerol). Suspension was passed through the High voltage Homogenizer (AVESTIN Company, EF-C3) for 4 times on ice, and the cells were lysed by the high pressure at around 120 MPa [24]. The lysate was centrifuged at 30,700g for 30 min at 4 °C to remove unbroken cells and debris. The supernatant was loaded onto a column with 2 mL Glutathione Sepharose resin (GE Healthcare) pre-equilibrated with Buffer A. The column was washed with 30–50 column volumes of Buffer A to remove unbound proteins and then incubated in 10 mL Buffer A

containing 30 $\mu g\,mL^{-1}$ Prescission Protease at 4 °C overnight to cut off GST tag. The next day, the flow through containing the untagged HadAB was collected, and desalted with six-fold dilusion with Buffer B (50 mM Tris–HCl, pH 8.0, 50 mM NaCl and 10% (v/v) glycerol). It was further purified using a 5 mL HiTrap™ Q HP anion exchange column (GE Healthcare) with an AKTA purifier (GE Healthcare) machine at 16 °C. The column was pre-equilibrated with Buffer B and the protein sample was loaded onto the column with 1.5 mL min^{-1} flow rate. After thorough washing with Buffer B for 2–3 column volumes, protein bound to the column was eluted with a linear gradient (0.05–0.5 M) of NaCl concentration in 8 column volumes with 1.5 mL min^{-1} flow rate. The linear gradient of NaCl concentration was created by mixing Buffer B and Buffer C (50 mM Tris–HCl, pH 8.0, 1 M NaCl and 10% (v/v) glycerol) by AKTA purifier machine. Fractions containing protein were analyzed by SDS–PAGE. Concentration of the separating gel and concentrating gel was 16% and 4%, respectively. Gels were stained with Coomassie R-250. Those fractions that contained pure target protein were pooled, desalted with Buffer B and then further purified by using a 1 mL RESOURCE™ Q anion exchange column (GE Healthcare). After processing in the same way, the pure target protein was pooled, concentrated to a volume less than 500 µL and injected into a 24 mL Superdex™ 75 10/300 GL gel-filtration column (GE Healthcare) pre-equilibrated with Buffer D (50 mM Tris–HCl, pH 8.0, 150 mM NaCl, and 10% (v/v) glycerol). The protein sample was eluted with 0.5 mL min^{-1} flow rate and collected by fractions. After SDS–PAGE analysis, fractions containing pure and homogenous HadAB was pooled and concentrated by ultrafiltration using Amicon centrifugal device (Millipore). The protein concentration was calculated by measuring the sample absorbance at 280 nm and adjusting with its extinction coefficient of 1.15. Purified HadAB was finally concentrated to 10 mg mL^{-1} for crystallization trials. The purification conditions of HadAB in each step was summarized in Table 1.

2.3. Crystallization

Initial crystallization screening was carried out at 16 °C by the hanging-drop vapor-diffusion method in 96-well plates (XtalQuest) using a Mosquito™ liquid-handling system (TPP Labtech). Each hanging drop was set up by mixing 200 nL protein solution (10 mg mL^{-1}) with 200 nL reservoir solution. The reservoir solutions were from commercially available crystallization screening kits (Index, SaltRx, PEG/Ion, PEG/Ion 2, Crystal Screen, Crystal Screen 2 and Natrix; Hampton Research). Crystals appeared in several conditions after a few days. Subsequent optimizations were carried out by varying the variety and concentration of polyethylene glycol (PEG), protein concentration and the pH of the reservoir solution. Final optimized crystals for data collection were obtained from a condition consisting of 6 mg mL^{-1} protein, 26% (w/v) PEG 4000, 100 mM HEPES, pH7.5.

2.4. Data collection and processing

Data collection was performed at 100 K on beamline BL17U at Shanghai Synchrotron Radiation Facility (SSRF) after crystals were soaked in the reservoir solution supplemented with 20% (v/v) glycerol for 10 s and flash frozen in liquid nitrogen. Crystals diffracted X-rays to 1.75 Å resolution and a data set was collected. HKL2000 [25] software was used for data processing.

3. Results and discussion

Our previous work indicated that, when HadB was expressed alone, most of the His-tagged product was inclusion body, and

the purified protein was relatively unstable in solution. Meanwhile, although HadAB complex could be obtained by a tandem expression method, we were unable to get high quality crystals from this sample by reason of the His-tag fused onto HadA. To improve our sample, co-expression was performed for GST tagged HadB and none tagged HadA. Purer HadAB complex was successfully overexpressed in *E. coli* and obtained. It is more conducive to crystallization and qualified diffraction data collection.

After expression, the protein was purified to homogeneity by utilizing a series of chromatographic techniques which included GST affinity purification at first using a Glutathione Sepharose column (GE Healthcare), ion exchange chromatography next using a HiTrap Q HP and a Resource Q anion-exchange column (GE Healthcare) and size-exclusion chromatography finally using a Superdex 75 10/300 GL gel filtration column (GE Healthcare). GST affinity chromatography could remove most of impure proteins. However, this process will lose a lot of target protein because of insufficient Prescission Protease digestion (Fig. 2). After two kinds of anion exchange chromatography purification, redundant HadA and most of the molecular chaperone could be separated (Fig. 3a and b). If either HiTrap™ Q HP or RESOURCE™ Q was used, even twice, purification effect will be reduced. Remarkably, the HadAB complex elution performed as a perfect single peak during gel filtration chromatography (Fig. 4). The final purity of sample after gel filtration as estimated by SDS–PAGE was >95%. An equal molar ratio of HadA and HadB for complex formation could be deduced from SDS–PAGE as well (Fig. 4). An elution peak volume of 9.3 mL corresponded to an approximate molecular mass of 65 kDa based on calibration of the column using standard molecular weight markers. Given the theoretical molecular weight of HadAB complex is 32.5 kDa, our result indicated that HadAB exists as a tetramer at 16 °C.

After initial crystallization screening, crystals were obtained in one of the conditions consisting of 22% (w/v) PEG 3000, 100 mM HEPES, pH7.5 after 2 days of incubation at 16 °C. After multiple optimization of crystallization conditions, crystals grew up to 50 μm (Fig. 5a). This crystal diffracted X-rays to 1.75 Å resolution on beamline BL17U at SSRF (Shanghai, China) (Fig. 5b). A data set was collected and the statistics of data collection are listed in Table 2. The crystal belonged to space group $P4_12_12$, with unit-cell parameters $a = b = 82.0$ Å, $c = 139.8$ Å, $\alpha = \beta = \gamma = 90.0°$. A Matthews coefficient of 3.56 $Å^3\ Da^{-1}$ [26,27], corresponding to a solvent content of 65.49%, indicated the presence of both one molecule of HadA and HadB per asymmetric unit.

In subsequent studies, an anomalous data set collected using crystals of selenomethionine labeled HadAB was used for phasing by single-wavelength anomalous diffraction (SAD) method. A total of four selenium sites were located by SHELX program suit [28] and the phase was solved. A density map was created by using intensities in the collected data and the solved phase. The 3D structural model of HadAB was built according to the density and refinement is currently in progress. Expectingly, the crystal structure of HadAB will help us understand the mechanism of substrate dehydration as well as biosynthesis of mycolic acids, and also lay the foundation for anti-TB drug discovery.

Conflict of interest

The authors declare that they have no conflict of interest.

Acknowledgements

References

[1] A. Zumla, A. George, V. Sharma, N. Herbert, I. Baroness, Masham of, WHO's 2013 global report on tuberculosis: successes, threats, and opportunities, Lancet 382 (2013) 1765–1767.

[2] WHO, Global tuberculosis report 2013, World Health Organization, Geneva, 2013.

[3] D.E. Goldberg, R.F. Siliciano, W.R. Jacobs Jr., Outwitting evolution: fighting drug-resistant TB, malaria, and HIV, Cell 148 (2012) 1271–1283.

[4] M. Jackson, M.R. McNeil, P.J. Brennan, Progress in targeting cell envelope biogenesis in *Mycobacterium tuberculosis*, Future Microbiol. 8 (2013) 855–875.

[5] C.M. Carel, K. Nukdee, S. Cantaloube, M. Bonne, C.T. Diagne, F.O. Laval, M. Didier, D. Zerbib, *Mycobacterium tuberculosis* proteins involved in mycolic acid synthesis and transport localize dynamically to the old growing pole and septum, PLoS One 9 (2014).

[6] K. Takayama, C. Wang, G.S. Besra, Pathway to synthesis and processing of mycolic acids in *Mycobacterium tuberculosis*, Clin. Microbiol. Rev. 18 (2005) 81–101.

[7] A. Bhatt, V. Molle, G.S. Besra, W.R. Jacobs Jr., L. Kremer, The *Mycobacterium tuberculosis* FAS-II condensing enzymes: their role in mycolic acid biosynthesis, acid-fastness, pathogenesis and in future drug development, Mol. Microbiol. 64 (2007) 1442–1454.

[8] Sylvain Cantaloube, Romain Veyron-Churlet, Nabila Haddache, Mamadou Daffe, D. Zerbib, The *Mycobacterium tuberculosis* FAS-II dehydratases and methyltransferases define the specificity of the mycolic acid elongation complexes, PLoS One 6 (2011).

[9] H. Marrakchi, M.A. Laneelle, M. Daffe, Mycolic acids: structures, biosynthesis, and beyond, Chem. Biol. 21 (2014) 67–85.

[10] J.W. Campbell, J.E. Cronan Jr., Bacterial fatty acid biosynthesis: targets for antibacterial drug discovery, Annu. Rev. Microbiol. 55 (2001) 305–332.

[11] E. Sacco, A.S. Covarrubias, H.M. O'Hare, P. Carroll, N. Eynard, T.A. Jones, T. Parish, M. Daffe, K. Backbro, A. Quemard, The missing piece of the type II fatty acid synthase system from *Mycobacterium tuberculosis*, Proc. Natl. Acad. Sci. USA 104 (2007) 14628–14633.

[12] Lian-Yong Gao, Francoise Laval, Elise H. Lawson, Richard K. Groger, J. Andy Woodruff, Hiroshi Morisaki, Jeffery S. Cox, Mamadou Daffe, E.J. Brown, Requirement for kasb in Mycobacterium mycolic acid biosynthesis, cell wall impermeability and intracellular survival: implications for therapy, Mol. Microbiol. 49 (2003) 1547–1563.

[13] A.K. Brown, A. Papaemmanouil, V. Bhowruth, A. Bhatt, L.G. Dover, G.S. Besra, Flavonoid inhibitors as novel antimycobacterial agents targeting Rv0636, a putative dehydratase enzyme involved in *Mycobacterium tuberculosis* fatty acid synthase II, Microbiology 153 (2007) 3314–3322.

[14] A.E. Grzegorzewicz, J. Kordulakova, V. Jones, S.E. Born, J.M. Belardinelli, A. Vaquie, V.A. Gundi, J. Madacki, N. Slama, F. Laval, J. Vaubourgeix, R.M. Crew, B. Gicquel, M. Daffe, H.R. Morbidoni, P.J. Brennan, A. Quemard, M.R. McNeil, M. Jackson, A common mechanism of inhibition of the *Mycobacterium tuberculosis* mycolic acid biosynthetic pathway by isoxyl and thiacetazone, J. Biol. Chem. 287 (2012) 38434–38441.

[15] P. Gratraud, N. Surolia, G.S. Besra, A. Surolia, L. Kremer, Antimycobacterial activity and mechanism of action of NAS-91, Antimicrob. Agents Chemother. 52 (2008) 1162–1166.

[16] V. Bhowruth, A.K. Brown, G.S. Besra, Synthesis and biological evaluation of NAS-21 and NAS-91 analogues as potential inhibitors of the mycobacterial FAS-II dehydratase enzyme Rv0636, Microbiology 154 (2008) 1866–1875.

[17] A.K. Brown, A. Bhatt, A. Singh, E. Saparia, A.F. Evans, G.S. Besra, Identification of the dehydratase component of the mycobacterial mycolic acid-synthesizing fatty acid synthase-II complex, Microbiology 153 (2007) 4166–4173.

[18] K. Bloch, Control mechanisms for fatty acid synthesis in Mycobacterium smegmatis, Adv. Enzymol Relat. Areas Mol. Biol. 45 (1977) 1–84.

[19] M.S. Kimber, F. Martin, Y. Lu, S. Houston, M. Vedadi, A. Dharamsi, K.M. Fiebig, M. Schmid, C.O. Rock, The structure of (3R)-hydroxyacyl-acyl carrier protein dehydratase (FabZ) from pseudomonas aeruginosa, J. Biol. Chem. 279 (2004) 52593–52602.

[20] D. Kostrewa, F.K. Winkler, G. Folkers, L. Scapozza, R. Perozzo, The crystal structure of PfFabZ, the unique beta-hydroxyacyl-ACP dehydratase involved in fatty acid biosynthesis of Plasmodium falciparum, Protein Sci. 14 (2005) 1570–1580.

[21] L. Zhang, W. Liu, T. Hu, L. Du, C. Luo, K. Chen, X. Shen, H. Jiang, Structural basis for catalytic and inhibitory mechanisms of beta-hydroxyacyl-acyl carrier protein dehydratase (FabZ), J. Biol. Chem. 283 (2008) 5370–5379.

[22] A.S. Kirkpatrick, T. Yokoyama, K.J. Choi, H.J. Yeo, Campylobacter jejuni fatty acid synthase II: structural and functional analysis of beta-hydroxyacyl-ACP dehydratase (FabZ), Biochem. Biophys. Res. Commun. 380 (2009) 407–412.

[23] M. Leesong, B.S. Henderson, J.R. Gillig, J.M. Schwab, J.L. Smith, Structure of a dehydratase-isomerase from the bacterial pathway for biosynthesis of unsaturated fatty acids: two catalytic activities in one active site, Structure 4 (1996) 253–264.

[24] Operating Instructions for the EmulsiFlex®-C3, AVESTIN, Inc., <http://www.medicinelab.org.il/website/FileLib/C3_Manual_English.pdf>.

[25] Z. Otwinowski, W. Minor, Processing of X-ray Diffraction Data Collected in Oscillation Mode, Elsevier, 1997. pp. 307–326.

[26] B.W. Matthews, Solvent content of protein crystals, J. Mol. Biol. 33 (1968) 491.

[27] E. Potterton, P. Briggs, M. Turkenburg, E. Dodson, A graphical user interface to the CCP4 program suite, Acta Crystallogr. D Biol. Crystallogr. 59 (2003) 1131–1137.

[28] T.R. Schneider, G.M. Sheldrick, Substructure solution with SHELXD, Acta Crystallogr. D Biol. Crystallogr. 58 (2002) 1772–1779.